

### Anguinomycins and Derivatives: Total Syntheses, Modeling, and Biological Evaluation of the Inhibition of Nucleocytoplasmic Transport

Simone Bonazzi,<sup>†,‡</sup> Oliv Eidam,<sup>\*,§</sup> Stephan Güttinger,<sup>||</sup> Jean-Yves Wach,<sup>†</sup>  
Ivo Zemp,<sup>||</sup> Ulrike Kutay,<sup>\*,||</sup> and Karl Gademann<sup>\*,†</sup>

Chemical Synthesis Laboratory (SB-ISIC-LSYNC), Swiss Federal Institute of Technology (EPFL),  
CH-1015 Lausanne, Switzerland, Department of Pharmaceutical Chemistry, University of  
California, San Francisco (UCSF), San Francisco, California 94158, and Institut für Biochemie,  
Swiss Federal Institute of Technology (ETHZ), CH-8093 Zürich, Switzerland

Received November 16, 2009; E-mail: karl.gademann@epfl.ch; oliv.eidam@ucsf.edu;  
ulrike.kutay@bc.biol.ethz.ch

**Abstract:** The preparation of the polyketide natural products anguinomycin C and D is reported based on key steps such as Negishi stereoinversion cross coupling, Jacobsen Cr(III)-catalyzed Hetero Diels–Alder reaction, Evans B-mediated syn-aldol chemistry, and B-alkyl Suzuki–Miyaura cross coupling. The configuration of both natural products was established as (5*R*,10*R*,16*R*,18*S*,19*R*,20*S*). Biological evaluation demonstrated that these natural products are inhibitors of the nuclear export receptor CRM1, leading to shutdown of CRM1-mediated nuclear protein export at concentrations above 10 nM. Analogues of anguinomycin and leptomycin B (LMB) have been prepared, and the simple  $\alpha,\beta$ -unsaturated lactone analogue **4** with a truncated polyketide chain retains most of the biological activity (inhibition above 25 nM). The structural basis for this inhibition has been demonstrated by modeling the transport inhibitors into X-ray crystal structures, thus highlighting key points for successful and strong biological action of anguinomycin and LMB.

#### Introduction

Natural products represent a major source of new drugs, and in particular related to anti-infective and anticancer agents, these metabolites account for roughly 50% of chemical entities on the pharmaceutical market.<sup>1</sup> In addition, derivatives obtained through synthetic organic chemistry have allowed one to leverage the potential of natural products by providing more effective and selective compounds.<sup>2</sup> These favorable properties of natural products have also led to their use as tool compounds in biology, as these efficient modulators of biological pathways enabled the generation of desired phenotypes in a well-controlled approach (chemical genetics).<sup>3</sup>

The leptomycin family of natural products features many of the desired properties regarding their use as clinical candidates or tool compounds.<sup>4</sup> Both leptomycin B (LMB)<sup>5</sup> (Figure 1) and

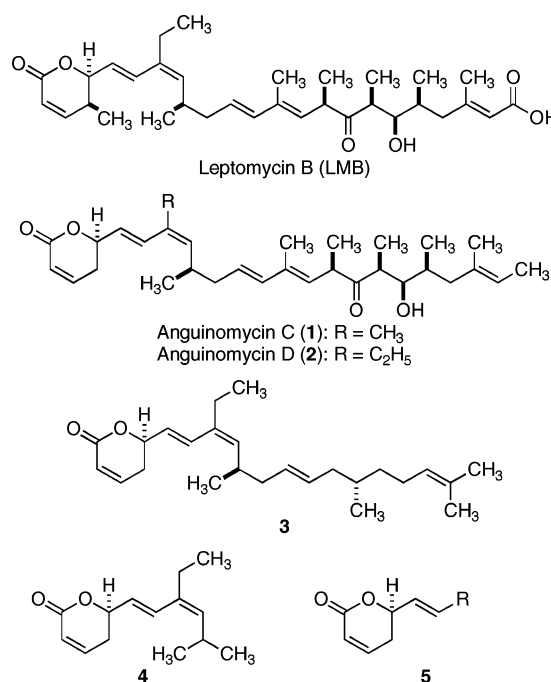


**Figure 1.** Leptomycin B (LMB), anguinomycins C (1), D (2), and derivatives 3 and 4 featuring the  $\alpha,\beta$ -unsaturated lactone 5.

callistatin<sup>6</sup> were identified and clinically evaluated<sup>7</sup> as potent anticancer agents. LMB was characterized as a potent inhibitor of the nuclear export of proteins,<sup>8</sup> and the mode of action

<sup>†</sup> EPFL.

<sup>‡</sup> Present address: Department of Chemistry and Chemical Biology, Harvard University, Cambridge, MA 02318.

<sup>§</sup> UCSF.

<sup>||</sup> ETHZ.

(1) (a) Newman, D. J.; Cragg, G. M. *J. Nat. Prod.* **2007**, *70*, 461–477.  
(b) Newman, D. J.; Cragg, G. M.; Snader, K. M. *J. Nat. Prod.* **2003**, *66*, 1022–1037.

(2) Newman, D. J.; Cragg, G. M. *J. Nat. Prod.* **2004**, *67*, 1216–1238.

(3) (a) Kaiser, M.; Wetzel, S.; Kumar, K.; Waldmann, H. *Cell. Mol. Life Sci.* **2008**, *65*, 1186–1201. (b) Burke, M. D.; Schreiber, S. L. *Angew. Chem., Int. Ed.* **2004**, *43*, 46–58.

(4) Kalesse, M.; Christmann, M. *Synthesis* **2002**, 981–1003.

(5) (a) Hamamoto, T.; Gunji, S.; Tsuji, H.; Beppu, T. *J. Antibiot.* **1983**, *36*, 639–645. (b) Hamamoto, T.; Seto, H.; Beppu, T. *J. Antibiot.* **1983**, *36*, 646–650.

involves binding to the chromosome maintenance region 1 (CRM1) exportin through its  $\alpha,\beta$ -unsaturated lactone moiety.<sup>9</sup> This leads to selective inhibition of the protein/protein interaction in the ternary CRM1-RAN-cargo protein complex<sup>10</sup> and thereby to efficient shutdown of CRM1-mediated nuclear protein export. High specificity and efficiency made LMB a frequently used tool compound in cell biology with over 1000 publications reporting its use.<sup>11</sup> This selective action also prompted the synthetic community, and many total syntheses of LMB and other members of this family have been reported.<sup>12</sup> Although initial studies on LMB were abandoned due to toxicity,<sup>7</sup> renewed clinical interest in LMB focused on its use in combination therapy (e.g., with gleevec)<sup>13</sup> and on the generation of less toxic

analogues with increased therapeutic windows by chemical modification<sup>14</sup> or conjugation to antibodies.<sup>15</sup>

Anguinomycins A–D were reported as selective agents targeting immortalized cells,<sup>16</sup> as they have been shown to induce apoptosis in pRB-inactivated tumor cells, while only inducing growth arrest in normal cells. This astonishing selectivity caused us to prepare totally synthetic anguinomycin C, and we were able to show that anguinomycin C is an inhibitor of CRM1-mediated nuclear export.<sup>17</sup> However, major questions concerning the mode of action of these compounds remain open. In particular, the role of the polyketide chain is unclear, as, for example, Kudo et al. suggested either mimicry of the protein cargo or induction of a conformational change of CRM1 by LMB.<sup>9a,b</sup> We wanted to investigate if this chain mimics the hydrophobic leucine-rich nuclear export signal of the cargo protein. It has been shown that interactions between this leucine-rich helical sequence and CRM1 are relatively weak, relying on Coulomb protein/protein interactions of a single helical fragment.<sup>11</sup> Therefore, we hypothesized that the side chain of LMB/anguinomycins can be either replaced by a simpler hydrophobic analogue or completely omitted.

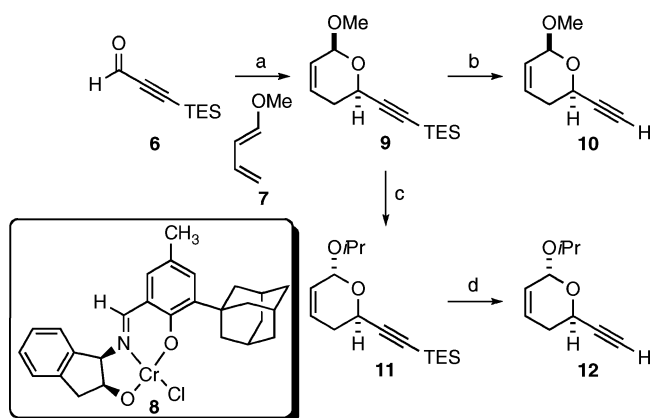
In this study, we investigate these hypotheses by a combination of synthetic chemistry, biological evaluation, and computational modeling. We report in full detail the total synthesis and biological evaluation of anguinomycins C (**1**) and D (**2**) as well as a series of analogues designed to probe these questions (Figure 1). We show that replacement of the side chain by a linear terpene is possible without strongly impacting biological activity (compound **3**), and we observed that analogue **4** with a truncated polyketide chain (Figure 1) almost fully retains biological activity. The structural basis for the biological activity of these natural products on CRM1 binding could be rationalized by atomistic modeling of LMB, anguinomycin, and general lactones of type **5** to CRM1.

## Results

**Total Syntheses of Anguinomycins C and D.** The synthesis of anguinomycins C (**1**) and D (**2**) started with the preparation of dihydropyran **9** via a hetero Diels–Alder reaction between known aldehyde **6**<sup>18</sup> and commercially available 1-methoxy-1,3-butadiene (**7**) (Scheme 1). The reaction was catalyzed by the Cr(III) catalyst (**8**) developed by Jacobsen and co-workers<sup>19</sup> and was carried out under solvent-free conditions and in the presence of 4 Å molecular sieves.<sup>20</sup> The dihydropyran **9** was obtained in high yield (86%), enantioselectivity (96% ee), and as a 5:1 diastereomeric mixture due to epimerization at the anomeric center under the reaction conditions. Attempts to directly use the MeO-protected lactol **9** for the continuation of the synthesis proved to be problematic. The diastereoisomers could be easily separated by chromatography, but after deprotection of the silyl group with TBAF, the resulting terminal alkyne **10** was volatile and difficult to handle. Therefore, we

- (6) Kobayashi, M.; Higuchi, K.; Murakami, N.; Tajima, H.; Aoki, S. *Tetrahedron Lett.* **1997**, *38*, 2859–2862.
- (7) Newlands, E. S.; Rustin, G. J. S.; Brampton, M. H. *Br. J. Cancer* **1996**, *74*, 648–649.
- (8) (a) Fornerod, M.; Ohno, M.; Yoshida, M.; Mattaj, I. W. *Cell* **1997**, *90*, 1051–1060. (b) Fukuda, M.; Asano, S.; Nakamura, T.; Adachi, M.; Yoshida, M.; Yanagida, M.; Nishida, E. *Nature* **1997**, *390*, 308–311. (c) Wolff, B.; Sanglier, J. J.; Wang, Y. *Chem. Biol.* **1997**, *4*, 139–147. (d) Nishi, K.; Yoshida, M.; Fujiwara, D.; Nishikawa, M.; Horinouchi, S.; Beppu, T. *J. Biol. Chem.* **1994**, *269*, 6320–6324.
- (9) (a) Kudo, N.; Wolff, B.; Sekimoto, T.; Schreiner, E. P.; Yoneda, Y.; Yanagida, M.; Horinouchi, S.; Yoshida, M. *Exp. Cell Res.* **1998**, *242*, 540–547. (b) Kudo, N.; Matsumori, N.; Taoka, H.; Fujiwara, D.; Schreiner, E. P.; Wolff, B.; Yoshida, M.; Horinouchi, S. *Proc. Natl. Acad. Sci. U.S.A.* **1999**, *96*, 9112–9117. (c) Daelemans, D.; Afonina, E.; Nilsson, J.; Werner, G.; Kjem, J.; De Clercq, E.; Pavlakis, G. N.; Vandamme, A. M. *Proc. Natl. Acad. Sci. U.S.A.* **2002**, *99*, 14440–14445. (d) Van Neck, T.; Pannecouque, C.; Vanstreels, E.; Stevens, M.; Dehaen, W.; Daelemans, D. *Bioorg. Med. Chem.* **2008**, *16*, 9487–9497.
- (10) (a) Dong, X.; Biswas, A.; Suel, K. E.; Jackson, L. K.; Martinez, R.; Gu, H.; Chook, Y. M. *Nature* **2009**, *458*, 1136–1141. (b) Dong, X.; Biswas, A.; Chook, Y. M. *Nat. Struct. Mol. Biol.* **2009**, *16*, 558–560. (c) Monecke, T.; Guttler, T.; Neumann, P.; Dickmanns, A.; Gorchich, D.; Ficner, R. *Science* **2009**, *324*, 1087–1091.
- (11) Review: Kutay, U.; Güttinger, S. *Trends Cell Biol.* **2005**, *15*, 121–124.
- (12) For callystatin, see: (a) Murakami, N.; Wang, W.; Aoki, M.; Tsutsui, Y.; Sugimoto, M.; Kobayashi, M. *Tetrahedron Lett.* **1998**, *39*, 2349–2352. (b) Crimmins, M. T.; King, B. W. *J. Am. Chem. Soc.* **1998**, *120*, 9084–9085. (c) Smith, A. B., III; Brandt, B. M. *Org. Lett.* **2001**, *3*, 1685–1688. (d) Kalesse, M.; Quitschalle, M.; Khandavalli, C. P.; Saeed, A. *Org. Lett.* **2001**, *3*, 3107–3109. (e) Marshall, J. A.; Bourbeau, M. P. *J. Org. Chem.* **2002**, *67*, 2751–2754. (f) Vicario, J. L.; Job, A.; Wolberg, M.; Müller, M.; Enders, D. *Org. Lett.* **2002**, *4*, 1023–1026. (g) Lautens, M.; Stammers, T. A. *Synthesis* **2002**, 1993–2012. (h) Langille, N. F.; Panek, J. S. *Org. Lett.* **2004**, *6*, 3203–3206. (i) Dias, L. C.; Meira, P. R. R. *J. Org. Chem.* **2005**, *70*, 4762–4773. (j) Reichard, H. A.; Rieger, J. C.; Micalizio, G. C. *Angew. Chem., Int. Ed.* **2008**, *47*, 7837–7840. (k) For leptomycin B, see: Kobayashi, M.; Wang, W.; Tsutsui, Y.; Sugimoto, M.; Murakami, N. *Tetrahedron Lett.* **1998**, *39*, 8291–8294. (l) For ratjadone, see: Christmann, M.; Bhatt, U.; Quitschalle, M.; Claus, E.; Kalesse, M. *Angew. Chem., Int. Ed.* **2000**, *39*, 4364–4366. (m) Williams, D. R.; Ihle, D. C.; Plummer, S. V. *Org. Lett.* **2001**, *3*, 1383–1386. (n) For leptofuranin D, see: Marshall, J. A.; Schaaf, G. M. *J. Org. Chem.* **2003**, *68*, 7428–7432. (o) For (–)-kazusamycin, see: Arai, N.; Chikaraishi, N.; Omura, S.; Kuwajima, I. *Org. Lett.* **2004**, *6*, 2845–2848. (p) For leptostatin, see: Marshall, J. A.; Mikowski, A. M.; Bourbeau, M. P.; Schaaf, G. M.; Valeriote, F. *Bioorg. Med. Chem. Lett.* **2006**, *16*, 320–323.
- (13) (a) Kancha, R. K.; Von Bubnoff, N.; Miething, C.; Peschel, C.; Götze, K. S.; Duyser, J. *Haematologica* **2008**, *93*, 1718–1722. (b) Aloisi, A.; Di Gregorio, S.; Stagno, F.; Guglielmo, P.; Mannino, F.; Sormani, M. P.; Bruzzi, P.; Gambacorti-Passerini, C.; Saglio, G.; Venuta, S.; Giustolisi, R.; Messina, A.; Vigneri, P. *Blood* **2006**, *107*, 1591–1598.
- (14) (a) Santi, D. V.; Zhou, Y. WO Patent 2005086944, 2005. (b) Santi, D. V.; Myles, D. C.; Dong, S.; Brian, H. U.S. Patent 2005272727, 2005. (c) Dong, S.; Santi, D. V. WO Patent 2007033214, 2007. (d) Dong, S.; Myles, D. C.; Santi, D. V.; Brian, H. CN Patent 1964718, 2008. (e) Mutka, S. C.; Yang, W. Q.; Dong, S. D.; Ward, S. L.; Craig, D. A.; Timmermans, P. B. M. W. M.; Murli, S. *Cancer Res.* **2009**, *69*, 510–517.

- (15) Bouchard, H.; Commercon, A.; Chari, R. V. J. E. WO Patent 2007144709, 2007.
- (16) (a) Hayakawa, Y.; Sohda, K. Y.; Shin-Ya, K.; Hidaka, T.; Seto, H. *J. Antibiot.* **1995**, *48*, 954–961. (b) Hayakawa, Y.; Adachi, K.; Komeshima, N. *J. Antibiot.* **1987**, *40*, 1349–1352.
- (17) Bonazzi, S.; Güttinger, S.; Zemp, I.; Kutay, U.; Gademann, K. *Angew. Chem., Int. Ed.* **2007**, *46*, 8707–8710.
- (18) Plater, M. J.; Aiken, S.; Bourhill, G. *Tetrahedron* **2002**, *58*, 2415–2422.
- (19) Chavez, D. E.; Jacobsen, E. N. *Org. Synth.* **2005**, *82*, 34–42.
- (20) Jarvo, E. R.; Lawrence, B. M.; Jacobsen, E. N. *Angew. Chem., Int. Ed.* **2005**, *44*, 6043–6046.

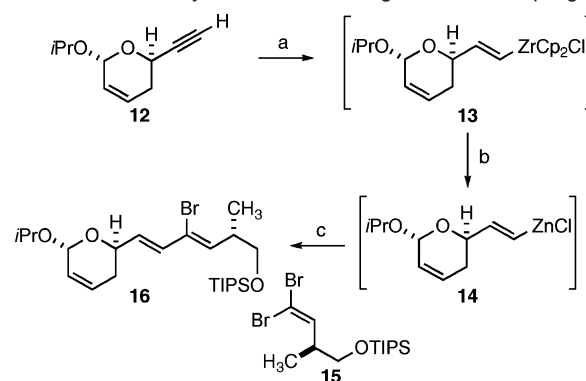
**Scheme 1.** Synthesis of the Terminal Alkyne **11** via a Hetero Diels–Alder Reaction<sup>a</sup>

<sup>a</sup> Reagents and conditions: (a) **7**, **8** (2.3 mol %), 4 Å MS, room temperature, 86%; 96% ee. (b) TBAF, THF, 0 °C → room temperature. (c) PTSA, *i*PrOH, room temperature, 86%. (d) TBAF (1 M in THF), THF, 0 °C → room temperature, 95%.

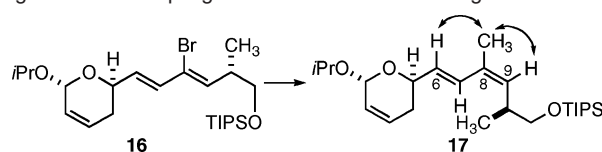
treated the diastereomeric mixture obtained in the Diels–Alder reaction under acidic conditions in *i*PrOH to afford the *i*PrO-protected lactol **11** as a single diastereoisomer in the thermodynamically more stable configuration. Deprotection with TBAF and purification on silicagel afforded the deprotected alkyne **12** as a colorless oil, which was carefully concentrated due to its volatility (Scheme 1).

We wanted to couple the terminal alkyne **12** to the dibromide **15** by a tandem hydrozirconation–Negishi cross-coupling reaction. Thus, the terminal alkyne **12** was hydrozirconated by Schwartz's reagent and the resulting species **13** transmetalated to the vinyl Zn species **14**. Separately, a yellow solution of Pd(PPh<sub>3</sub>)<sub>4</sub> (5 mol %) in THF was treated with a solution of DIBAH (10 mol %) to give a dark red solution. After 30 min, the readily available dibromoolefin **15**<sup>21</sup> in THF was added, and the resulting mixture was transferred into the separately prepared vinylzinc solution of **14**. The mixture was stirred 10 h at 40 °C, and after workup and purification, the coupled (*E*)-product **16** was obtained in 81% yield as a single diastereoisomer (Scheme 2). <sup>1</sup>H NMR and NOE spectroscopic analyses of product **16** confirmed that the reaction had occurred in a completely selective fashion, resulting in the (6*E*,8*Z*) isomer.

This Negishi cross-coupling between alkyne **12** and dibromoolefin **15** afforded the coupled trans Br-olefin **16**, but for the preparation of anguinomycins C and D a *cis* configuration of the double bond at C(8)–C(9) was required. To achieve this goal, we applied the procedure developed by Negishi and co-workers,<sup>22</sup> allowing the installation of the alkyl residue at C(8) with inversion of the configuration of the double bond. The nature of the catalyst employed in the Pd-catalyzed alkenylation of alkenyl halide influences the selectivity of the resulting product.<sup>22</sup> This reaction can occur with retention or inversion of the configuration depending on the ligands on Pd. As in the first Negishi cross coupling, the trans product **16** was obtained, and an inversion of the configuration affording the *cis* product (6*E*,8*Z*) as present in the anguinomycin structure was required. In addition, by employing either Me<sub>2</sub>Zn or Et<sub>2</sub>Zn in the Negishi

**Scheme 2.** Tandem Hydrozirconation–Negishi Cross-Coupling<sup>a</sup>

<sup>a</sup> Reagents and conditions: (a) Cp<sub>2</sub>ZrHCl, 0 °C → room temperature, THF, 1 h. (b) ZnCl<sub>2</sub>, THF, room temperature, 30 min. (c) **15**, Pd(PPh<sub>3</sub>)<sub>4</sub> (5 mol %), DIBAH (1.0 M in hexane), room temperature → 40 °C, 13 h, 81%.

**Scheme 3.** Synthesis of Fragment **17** of Anguinomycin C via Negishi Cross-Coupling with Inversion of the Configuration<sup>a</sup>

<sup>a</sup> Reagents and conditions: Pd(PPh<sub>3</sub>)<sub>4</sub> (10 mol %), Me<sub>2</sub>Zn (2.0 M in toluene), THF, 45 °C, 38 h, 68%, *cis*/*trans* > 97:3. Arrows in **17** indicate NOE correlations.

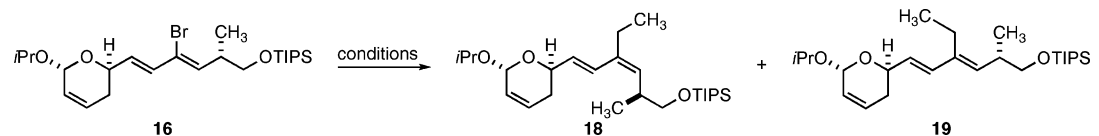
coupling, we would be able to access both anguinomycins C and D, respectively. We started with the preparation of the intermediate for the synthesis of anguinomycin C by adding Me<sub>2</sub>Zn (2 M in toluene) to a solution of Br-diene **16** and Pd(PPh<sub>3</sub>)<sub>4</sub> (10 mol %) in THF under argon atmosphere. The resulting orange-colored solution was stirred for 24 h at 45 °C, then a second addition of Me<sub>2</sub>Zn was added, and complete conversion of the starting material was achieved after an additional 14 h. As expected, the use of Pd(PPh<sub>3</sub>)<sub>4</sub> afforded the *cis* product **17** (assigned by NOEs) as a single isomer in 68% yield (Scheme 3).

The same Negishi cross coupling with stereoinversion reaction was adopted for the synthesis of the fragment for anguinomycin D. In this case, we used Et<sub>2</sub>Zn (1.5 M in toluene), which was added to a solution of alkenylhalide **16** and Pd(PPh<sub>3</sub>)<sub>4</sub> (10 mol %) in THF. However, following workup we obtained a mixture of unreacted starting material, and the *cis* and *trans* products. Separation of the two isomers by chromatography on SiO<sub>2</sub> was unsuccessful, as the similar polarity of the *cis* and *trans* isomer did not allow the isolation of the pure desired isomer. Attempts to force the reaction by adding more Et<sub>2</sub>Zn were unsuccessful and promoted formation of the undesired *trans* isomer. Generally, it was found that varying amounts of O<sub>2</sub> present in the solvents led to mixed results, and degassing the solvent (three freeze/pump/thaw cycles) gave better results. The *cis* product was identified as the major isomer by using Pd(PPh<sub>3</sub>)<sub>4</sub> and Et<sub>2</sub>Zn, but conversion of the starting material was not complete and formation of the *trans* compound was still observed. At this point, we chose to screen several different Pd catalysts (5–10 mol %) for the reaction (Table 1). The screened catalysts were Pd(PPh<sub>3</sub>)<sub>4</sub>, PdCl<sub>2</sub>(dppf), Pd(P<sup>*t*</sup>Bu)<sub>3</sub>, PdCl<sub>2</sub>(DPEphos), *trans*-di(*μ*-acetato)bis[*o*-(tolyl-phosphino)benzyl] dipalladium(II), and allyl[1,3-bis(mesityl)imidazol-2-ylidene] Pd chloride. In agreement with data reported by Negishi and co-workers,<sup>22a</sup>

(21) Komatsu, K.; Tanino, K.; Miyashita, M. *Angew. Chem., Int. Ed.* **2004**, 43, 4341–4345.

(22) (a) Zeng, X.; Hu, Q.; Qian, M.; Negishi, E. I. *J. Am. Chem. Soc.* **2003**, 125, 13636–13637. (b) Zeng, X.; Qian, M.; Hu, Q.; Negishi, E. I. *Angew. Chem., Int. Ed.* **2004**, 43, 2259–2263.



**Table 1.** Screening of Conditions for the Preparation of Fragment **18** of Anguinomycin D via Negishi Cross-Coupling with Selective Retention or Inversion of the Configuration<sup>a</sup>


catalyst	equivalents (mol %)	concentration (M vs <b>16</b> )	reaction time (h)	ratio <sup>a</sup>	yield (%)
Pd(PPh <sub>3</sub> ) <sub>4</sub>	5	0.06	24	0.14/1.00/0.38	n.d.
Pd(PPh <sub>3</sub> ) <sub>4</sub>	10	0.1	28	0.16/1.00/0.17	n.d.
PdCl <sub>2</sub> (dppf)	10	0.05	20	1.00/1.08/0.66	n.d.
Pd(PtBu <sub>3</sub> ) <sub>2</sub> <sup>b</sup>	10	0.05	3.5	0/0/1.00	75%
PdCl <sub>2</sub> (DPEphos) <sup>c</sup>	5	0.08	14	0/1.00/0	84%
PdCl <sub>2</sub> (DPEphos) <sup>c</sup>	10	0.08	14	0/1.00/0	84%
<i>trans</i> -di( $\mu$ -acetato)bis[ <i>o</i> -(tolylphosphino)benzyl] dipalladium(II) <sup>d</sup>	10	0.05	20	0/0/1.00	65%
allyl[1,3-bis(mesityl)imidazol-2-ylidene] palladium chloride <sup>b</sup>	10	0.05	20	0/0/1.00	77%

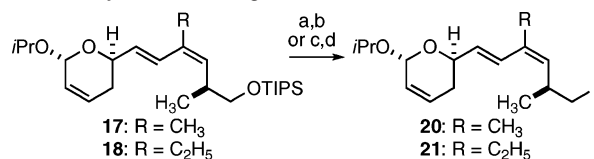
<sup>a</sup> The ratio of **16**/**18**/**19** is reported. <sup>b</sup> During the addition of Et<sub>2</sub>Zn, the solution turned immediately to a dark-brown color. <sup>c</sup> During all of the reactions, the solution maintained an orange-red color. <sup>d</sup> At ca. 35 °C, the solution turned to a dark-brown color.

PdCl<sub>2</sub>(DPEphos) revealed to be the best catalyst to achieve alkenylation with inversion of configuration. The *cis* adduct **18**, the intermediate for the synthesis of anguinomycin D, was obtained in 84% yield as a single isomer. The reaction proved to be clean, without traces of remaining starting material or the undesired *trans* isomer. It is probably the higher thermal stability of PdCl<sub>2</sub>(DPEphos) as compared to Pd(PPh<sub>3</sub>)<sub>4</sub> that made the catalyst efficient over a longer time without any decomposition. The percentage of the catalyst employed (5 or 10 mol %) did not influence the yield and selectivity of the reaction, affording in both cases only the *cis* isomer. We have found that both Pd(PPh<sub>3</sub>)<sub>4</sub> and PdCl<sub>2</sub>(dppf) resulted in mixtures of *cis* and *trans* products. In addition to the previously reported Pd(PtBu<sub>3</sub>)<sub>2</sub>, the *trans*-di( $\mu$ -acetato)bis[*o*-(tolylphosphino)benzyl] dipalladium(II) and the allyl[1,3-bis(mesityl)imidazol-2-ylidene] Pd chloride also afforded exclusively the *trans* adduct **19**, via retention of configuration and moderate to good yields.

By using the Negishi cross coupling with selective inversion of configuration, a straightforward and effective route to the trisubstituted C(8)–C(9) olefin in **18** and **19** was identified. It should be pointed out that the reverse strategy, that is, reacting the dibromoolefin **15** with Me<sub>2</sub>Zn or MeB(OH)<sub>2</sub> under Negishi or Suzuki conditions, was evaluated but proved to be troublesome as low yields and selectivities were observed. In addition, the use of the TIPS group for the primary OH group was necessary, as the TBS group was found to be unstable under the Negishi conditions.

At this point, the silyl group of both **17** and **18** was removed by treatment with TBAF in THF, affording the deprotected products in quantitative yield. Subsequently, both alcohols were treated with I<sub>2</sub>, PPh<sub>3</sub>, and imidazole in toluene to obtain the alkyl iodide products **20** and **21** in good yields (Scheme 4).

The synthesis of the polyketide chain was based on the classic Evans *syn*-aldol strategy,<sup>23</sup> but we chose to employ the DIOZ auxiliary (DIOZ = 4-isopropyl-5,5-diphenyloxazolidin-2-one) developed by Seebach and Hintermann.<sup>24</sup> The additional Ph groups on the auxiliary increase the stability against nucleophilic attack, thus allowing, for example, the formation of the lithiated

**Scheme 4.** Synthesis of Fragments **20** and **21**<sup>a</sup>

<sup>a</sup> Reagents and conditions: From **17** to **20**, (a) TBAF (1.0 M in THF), THF, 0 °C → room temperature, 2 h, 99%. (b) PPh<sub>3</sub>, imidazole, I<sub>2</sub>, toluene/Et<sub>2</sub>O, 0 °C → room temperature, 2 h, 75%. From **18** to **21**, (c) TBAF (1.0 M in THF), THF, 0 °C → room temperature, 1.5 h, 98%. (d) PPh<sub>3</sub>, imidazole, I<sub>2</sub>, toluene/Et<sub>2</sub>O, 0 °C, 45 min, 89%.

oxazolidinone by using *n*BuLi at 0 °C. Moreover, the presence of the two Ph groups increases the selectivity of the reactions as well as the crystallinity of the resulting products. This auxiliary demonstrated its utility in total synthesis when being used by chemists at Novartis in the synthesis of discodermolide.<sup>25</sup> We sought the all-*syn* configuration of the polyketide chain, due to the structural similarity of anguinomycin to LMB. In addition, we chose to keep the hydroxy group at C(17) unprotected for the entire synthesis, based on reports by Dias and Meira.<sup>12i</sup> Treatment of the known acylated chiral auxiliary **22**<sup>24a</sup> with LDA generated the lithium enolate, which reacted via enantioselective alkylation with allylic bromide **23**<sup>26</sup> to give the adduct **24** in high yield (92%) and excellent selectivity (dr > 97:3) as a crystalline white solid. The auxiliary was removed with LAH in quantitative yield, which allowed for the recycling of the cleaved oxazolidinone and Swern oxidation of the intermediate gave the aldehyde **25**. A stereoselective B-mediated aldol reaction was carried out by treatment of *ent*-**22** with Bu<sub>2</sub>BOTf following addition of aldehyde **25**.<sup>27</sup> The aldol **26** was obtained in 77% yield and a diastereomeric ratio of 87:13 (Scheme 5), which is comparable to the selectivities achieved by other groups using similar substrates.<sup>12a</sup> The two diastereoisomers displayed similar *R<sub>f</sub>* values, but separation by repeated flash chromatography on SiO<sub>2</sub> was possible, affording pure *syn*-aldol **26**.

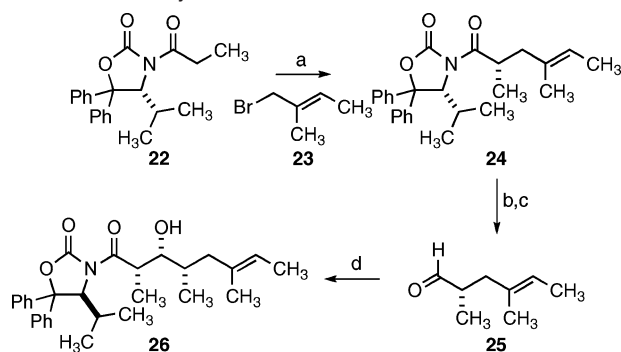
(23) Evans, D. A.; Bartroli, J.; Shih, T. L. *J. Am. Chem. Soc.* **1981**, *103*, 2127–2129.

(24) (a) Hintermann, T.; Seebach, D. *Helv. Chim. Acta* **1998**, *81*, 2093–2126. (b) Bull, S. D.; Davies, S. G.; Garner, A. C.; Kruchinin, D.; Key, M. S.; Roberts, P. M.; Savory, E. D.; Smith, A. D.; Thomson, J. E. *Org. Biomol. Chem.* **2006**, *4*, 2945–2964.

(25) (a) Loiseleur, O.; Koch, G.; Wagner, T. *Org. Process Res. Dev.* **2004**, *8*, 597–602. (b) Loiseleur, O.; Koch, G.; Cercus, J.; Schürch, F. *Org. Process Res. Dev.* **2005**, *9*, 259–271.

(26) Katzenellenbogen, J. A.; Crumrine, A. L. *J. Am. Chem. Soc.* **1976**, *98*, 4925–4935.

(27) For *ent*-**25**, see: White, J. D.; Johnson, A. T. *J. Org. Chem.* **1994**, *59*, 3347–3358.

**Scheme 5.** The Alkylation and the First Aldol Reaction<sup>a</sup>

<sup>a</sup> Reagents and conditions: (a) **22**, LDA, -78 °C, 30 min, then **23**, THF, -78 °C → -10 °C, 26 h, 92%, dr > 97:3. (b) LAH, Et<sub>2</sub>O, 0 °C → room temperature, 3.5 h, quant. (c) Oxalyl chloride, DMSO, CH<sub>2</sub>Cl<sub>2</sub>, -78 °C, then NEt<sub>3</sub>, -78 °C → 0 °C, 50 min, 99%. (d) *ent*-**22**, Bu<sub>3</sub>BOTf (1.0 M in CH<sub>2</sub>Cl<sub>2</sub>), NEt<sub>3</sub>, -5 °C, 1 h, then -78 °C, **25**, CH<sub>2</sub>Cl<sub>2</sub>, -78 °C → 0 °C, 2 h, 77%, dr > 87:13.

The *syn*-aldol **26** was transformed to the Weinreb amide **27** in good yield (86%) following standard procedures. Amide **27** could be crystallized in hexane, and the all-*syn* configuration was confirmed by X-ray crystallographic analysis (Scheme 6). Protection of the alcohol with TBS and treatment with DIBAH gave aldehyde **28** in excellent yield. A second B-mediated aldol reaction using the same auxiliary, *ent*-**22**, and aldehyde **28** afforded the *syn*-aldol adduct **29** in excellent diastereoselectivity (dr > 97:3) and 61% yield. Attempts to convert *syn*-aldol **29** to the Weinreb amide **30** proved to be difficult, and even under forcing reaction conditions, the product **30** was only obtained in 41% yield. Therefore, we sought to exploit a strength of the DIOZ auxiliary with its sterically protected carbamate C=O group and directly cleave the imide by using LAH. Thus, the *syn*-aldol **29** could be directly converted to the aldehyde **31**. A Wittig reaction between aldehyde **31** and (carbethoxyethylidene)-triphenylphosphorane afforded the  $\alpha,\beta$ -unsaturated ester **32** in excellent yield (99%) as a single isomer. Reduction with DIBAH to the alcohol and subsequent MnO<sub>2</sub> oxidation gave the  $\alpha,\beta$ -unsaturated aldehyde **33** in 80% yield over two steps. Aldehyde **33** (mp = 75–77 °C) was crystallized from hexane, and X-ray crystallographic analysis allowed for the unambiguous determination of the relative configuration of the polyketide chain (Scheme 6). The transformation of the aldehyde **33** to the vinyl iodide **34** via a Takai reaction was initially expected to be problematic due to selectivity issues of this reaction when using an  $\alpha$ -substituted  $\alpha,\beta$ -unsaturated aldehyde.<sup>28</sup> For example, recently Lipshutz and co-workers reported that a similar aldehyde was found to be troublesome, and chose to carry out a three-step replacement for the Takai reaction.<sup>29</sup> In our case, the vinyl iodide **34** was smoothly prepared in excellent yield and selectivity (dr > 97:3) (Scheme 6). At the same time, we also prepared a derivative of polyketide chain featuring a TMS protected hydroxy group at C(17) to evaluate the differences from the unprotected version in the  $sp^3$ – $sp^2$  Suzuki cross coupling. Thus, the  $\alpha,\beta$ -unsaturated ester **32** was protected with TMSCl in 77% yield, and subsequent reduction of this substrate with DIBAH gave the corresponding alcohol, which was oxidized using Swern conditions to afford aldehyde **35** in

quantitative yield. Takai reaction afforded the all-protected vinyl iodide **36** in 88% yield and in an *E/Z* ratio of 95:5 (Scheme 6).

Having all of the fragments in hand, we attempted the  $sp^3$ – $sp^2$  Suzuki cross coupling following Johnson's conditions<sup>30</sup> previously used by Marshall and co-workers in the synthesis of callistatin.<sup>12e</sup> The alkyl iodide **20** was reacted with 9-MeO-9-BBN and *t*BuLi at -78 °C, forming the boronate intermediate **37**, to which a solution containing vinyl iodide **34**, Cs<sub>2</sub>CO<sub>3</sub>, AsPh<sub>3</sub>, and PdCl<sub>2</sub>(dppf) in a DMF/water mixture was added. The reaction proceeded smoothly, and the coupled product **39** featuring the complete skeleton of anguinomycin C was isolated in 80% yield (Scheme 7).<sup>31</sup> The same procedure was applied to the fully protected vinyl iodide **36** and boronate intermediate **37**. However, this reaction proved to be problematic, and the coupled product **40** was obtained only in low yield (Scheme 7). Having confirmed the superiority, in terms of yield, of the vinyl iodide **34** with the free hydroxy group at C(17) in the  $sp^3$ – $sp^2$  Suzuki cross coupling, we performed the reaction with compound **34** for the preparation of the anguinomycin D skeleton. Alkyl iodide **21** was converted to the boronate intermediate **38**, which was coupled to vinyl iodide **34** under the same conditions. As expected, the reaction proceeded smoothly, but during purification on SiO<sub>2</sub> the appearance of a side product was observed. Two fractions were collected, one of which the pure coupled product **41** in 48% yield could be characterized, and the second fraction appeared to contain product **41** and a minor side compound (Scheme 7). It was decided to separately use both fractions in the next steps.

Final steps for completion of the total syntheses were then performed. Thus, treatment of product **39** under acidic conditions (PPTS) in a mixture of acetone/water cleaved the acetal in 95% yield to give the corresponding lactol. Surprisingly, attempted DMP oxidation of the lactol only oxidized the OH group on the polyketide chain and did not form the lactone from the starting lactol. A further oxidation step using MnO<sub>2</sub> was then required to furnish lactone **42** in modest yield (47% over two steps). Finally, the TBS group was removed using HF·pyridine buffered with pyridine, which proved to be crucial in avoiding degradation of the product. After workup, the crude mixture was directly purified by semipreparative HPLC to afford anguinomycin C (**1**) in 82% yield (Scheme 8).

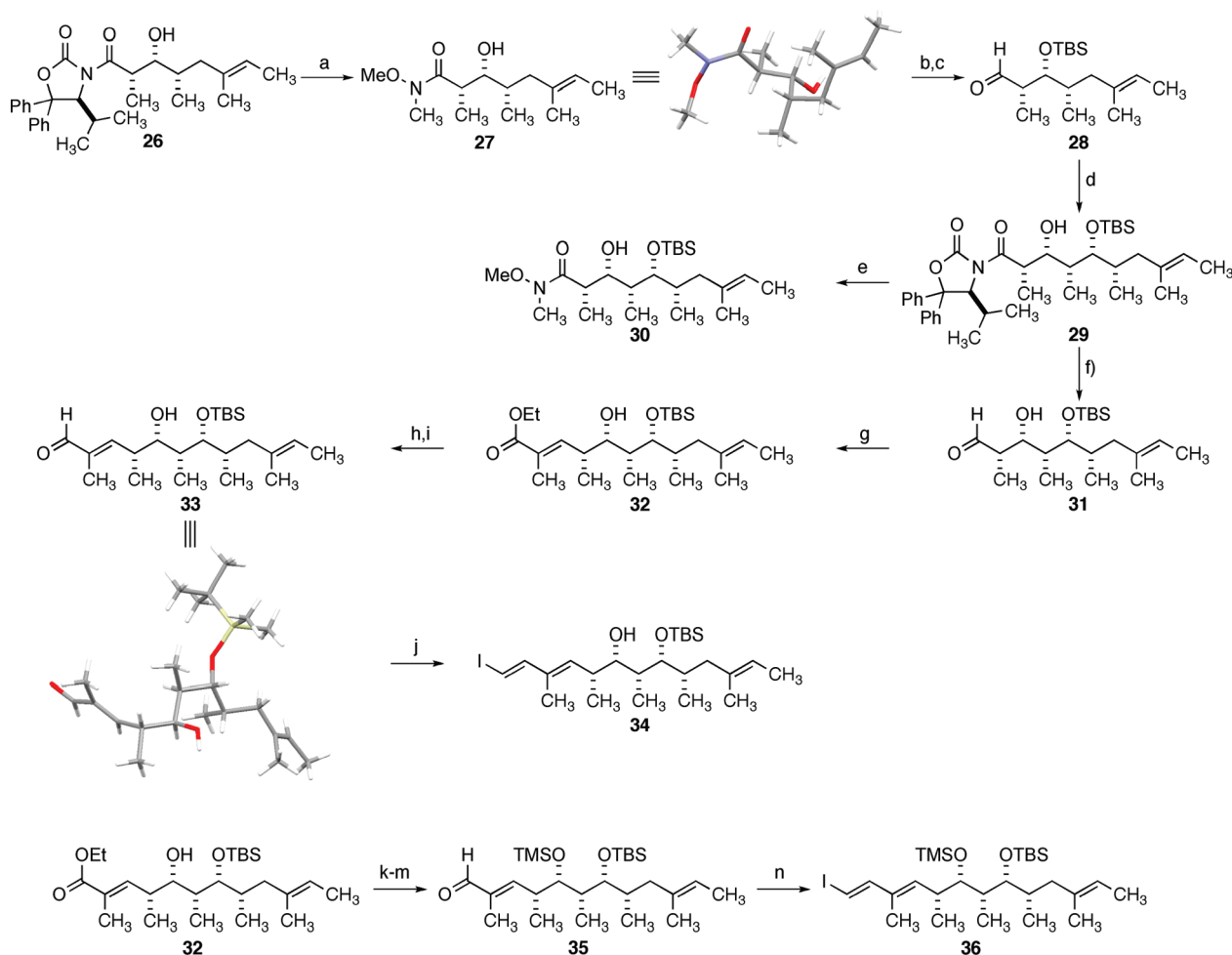
A similar procedure was adopted for the final transformation of intermediate **41** to anguinomycin D. Acid-catalyzed cleavage of the acetal in product **41** afforded the corresponding lactol in good yield. Because of the poor yield obtained during the two-step oxidation (DMP and MnO<sub>2</sub>) for the formation of compound **42** in the synthesis of anguinomycin C (**1**), we chose to use PCC for the oxidation of both the alcohol at C(17) and the lactol. The oxidation was successful and afforded lactone **43**, which was directly treated with HF·pyridine solution buffered with pyridine for the final deprotection. This time, to avoid the aqueous workup, we cooled the reaction to 0 °C and added some SiO<sub>2</sub> to the reaction to quench the excess of HF·pyridine. The resulting mixture was then loaded directly onto a column of SiO<sub>2</sub> and chromatographed, affording anguinomycin D (**2**) in 60% yield (over two steps) (Scheme 8).

(28) (a) Takai, K.; Nitta, K.; Utimoto, K. *J. Am. Chem. Soc.* **1986**, *108*, 7408–7410. (b) Okazoe, T.; Takai, K.; Utimoto, K. *J. Am. Chem. Soc.* **1987**, *109*, 951–953.

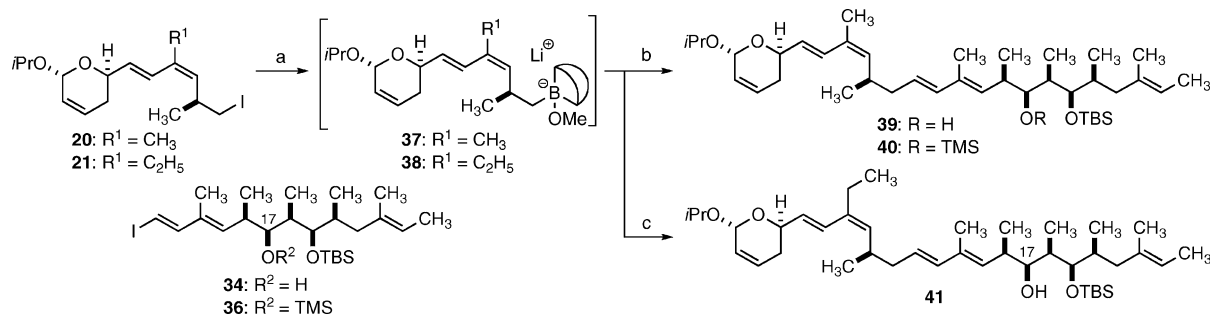
(29) Lipshutz, B. H.; Amorelli, B. *J. Am. Chem. Soc.* **2009**, *131*, 1396–1397.

(30) Johnson, C. R.; Braun, M. P. *J. Am. Chem. Soc.* **1993**, *115*, 11014–11015.

(31) Unsuccessful results for the cross-coupling of similar substrates using K<sub>3</sub>PO<sub>4</sub> instead of Cs<sub>2</sub>CO<sub>3</sub> and AsPh<sub>3</sub> were reported by Chakraborty and co-workers: Chakraborty, T. K.; Goswami, R. K.; Sreekanth, M. *Tetrahedron Lett.* **2007**, *48*, 4075–4078.

**Scheme 6.** The Second Aldol and the Takai Reaction<sup>a</sup>

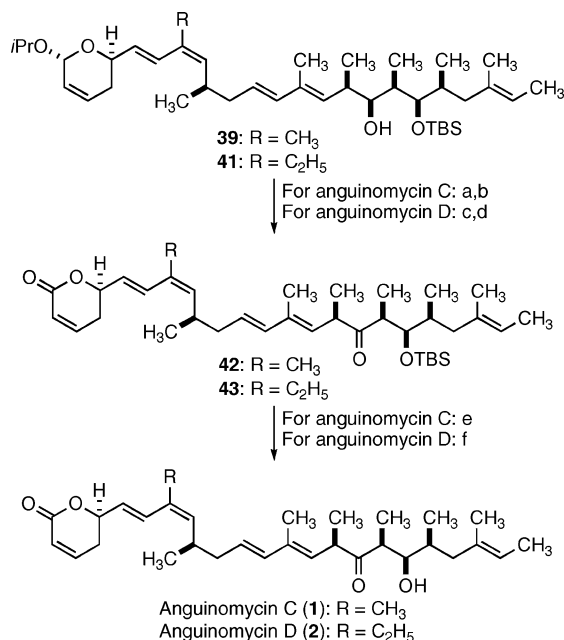
<sup>a</sup> Reagents and conditions: (a) MeONHMe·HCl, AlMe<sub>3</sub>, CH<sub>2</sub>Cl<sub>2</sub>, 0 °C → room temperature, then **26**, CH<sub>2</sub>Cl<sub>2</sub>, 0 °C → room temperature, 15 h, 86%. (b) TBSOTf, 2,6-lutidine, −20 °C → 0 °C, 1 h, 99%. (c) DIBAH (1 M in hexane), THF, −78 °C, 1 h, quant. (d) *ent*-**22**, Bu<sub>2</sub>BOTf (1 M in CH<sub>2</sub>Cl<sub>2</sub>), NEt<sub>3</sub>, −5 °C, 45 min, then −78 °C, **28**, CH<sub>2</sub>Cl<sub>2</sub>, −78 °C → 0 °C, 3 h, 61%, dr > 97:3. (e) MeONHMe·HCl, AlMe<sub>3</sub>, CH<sub>2</sub>Cl<sub>2</sub>, 0 °C → room temperature, then **29**, CH<sub>2</sub>Cl<sub>2</sub>, 0 °C → room temperature, 68 h, 41%. (f) LAH (1 M in Et<sub>2</sub>O), toluene, −17 °C, 20 min, 83%. (g) **31**, toluene, then (carbethoxyethylidene)triphenylphosphorane, room temperature → 35 °C, 5 h, 99%, dr > 97:3. (h) DIBAH (1.0 M in hexane), THF, −78 °C → −10 °C, 1.5 h, 93%. (i) MnO<sub>2</sub>, CH<sub>2</sub>Cl<sub>2</sub>, room temperature, 2.5 h, 86%. (j) CrCl<sub>2</sub>, CHI<sub>3</sub>, THF, 0 °C, 2 h, quant., dr > 97:3. (k) TMSCl, DMAP, NEt<sub>3</sub>, CH<sub>2</sub>Cl<sub>2</sub>, 0 °C, 1 h, 77%. (l) DIBAH (1.0 M in hexane), CH<sub>2</sub>Cl<sub>2</sub>, −78 °C, 1 h, quant. (m) MnO<sub>2</sub>, CH<sub>2</sub>Cl<sub>2</sub>, room temperature, 3.5 h, quant. (n) CrCl<sub>2</sub>, CHI<sub>3</sub>, THF, 0 °C, 2.5 h, 88%, dr > 95:5.

**Scheme 7.** The sp<sup>3</sup>–sp<sup>2</sup> 9-MeO-9-BBN-Mediated Suzuki Cross-Coupling<sup>a</sup>

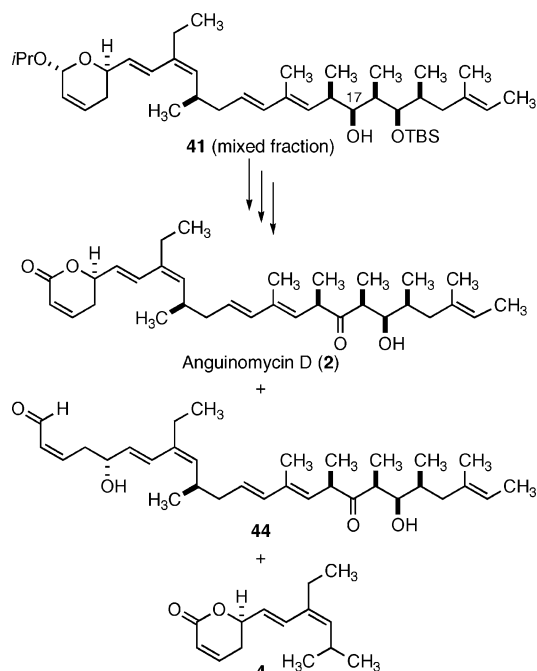
<sup>a</sup> Reagents and conditions: (a) **20** (respectively **21**), 9-MeO-9-BBN (1.0 M in hexane), *t*BuLi (1.5 M in pentane), Et<sub>2</sub>O, then THF, −78 °C → room temperature, 1 h. (b) **34** (respectively **36**), Pd(dppf)Cl<sub>2</sub>·CH<sub>2</sub>Cl<sub>2</sub> (5 mol %), AsPh<sub>3</sub> (15 mol %), CsCO<sub>3</sub>, H<sub>2</sub>O, DMF, then **37**, room temperature, overnight, 80% (respectively 34%). (c) **34**, Pd(dppf)Cl<sub>2</sub>·CH<sub>2</sub>Cl<sub>2</sub> (5 mol %), AsPh<sub>3</sub> (15 mol %), CsCO<sub>3</sub>, H<sub>2</sub>O, DMF, then **38**, room temperature, 20 h, 48%.

A second reaction batch containing a mixture of product **41** and a minor byproduct was subjected to the same sequence. Thus, acid-promoted cleavage of the acetal, oxidation using PCC, and final removal of the silyl protecting group afforded a mixture of products that were purified by chromatography on SiO<sub>2</sub>. Three compounds were isolated, anguinomycin D (**2**), the

α,β-unsaturated aldehyde **44**, and trace amounts of compound **4** (Scheme 9). Aldehyde **44** results from opening of the lactone ring, a problem also encountered by Lautens and co-workers in their synthesis of callistatin.<sup>12g</sup> Compound **4** probably originated from degradation of the boronate intermediate in the Suzuki reaction.

**Scheme 8.** Completion of the Total Syntheses of Anguinomycins C (1) and D (2)<sup>a</sup>

<sup>a</sup> Reagents and conditions: For anguinomycin C, (a) PPTS, acetone/water (3:1), room temperature, 22 h, 95%. (b) (i) DMP, CH<sub>2</sub>Cl<sub>2</sub>, room temperature, 4 h; (ii) MnO<sub>2</sub>, CH<sub>2</sub>Cl<sub>2</sub>, room temperature, 14 h, 47%. (e) HF·pyridine, pyridine, room temperature, 4.5 days, 82%. For anguinomycin D, (c) PPTS, acetone/water (5/1), room temperature, 22 h, 91%. (d) PCC, 4 Å MS, AcOH, CH<sub>2</sub>Cl<sub>2</sub>, room temperature, 1.5 h. (f) HF·pyridine, pyridine, room temperature, 4.5 days, 60% (two steps).

**Scheme 9.** Compounds Generated by Using a Mixture of Diastereoisomers at C(17)

Both anguinomycins C (1) and D (2) were isolated as colorless oils, and their optical rotation values, the UV traces, and IR spectra of the synthetic products match with those reported in the literature,<sup>16a</sup> and the high resolution ESI confirmed the correct masses. The NMR spectroscopic data of synthetic anguinomycins C and D were identical to those reported in the literature<sup>16a</sup> (see Supporting Information), except

that for anguinomycin C, the proton of the OH group at C(17) was not reported in the original isolation report, but was identified in the <sup>1</sup>H NMR spectrum of the synthetic sample (2.40 ppm). It is generally assumed that compounds as complex as the anguinomycins are unstable due to the  $\alpha,\beta$ -unsaturated lactone, the deconjugated diene, or potential epimerization. In our laboratory, anguinomycin C could be stored at  $-20\text{ }^{\circ}\text{C}$  for more than 1 year without decomposition. Moreover, anguinomycins C and D are soluble in EtOH and could be stored as a solution at  $-20\text{ }^{\circ}\text{C}$  for several months without decomposition (as assessed by HPLC).

**Biological Evaluation as Inhibitors of Nucleocytoplasmic Transport.** Compounds such as LMB selectively inhibit the CRM1-mediated nucleocytoplasmic transport by blocking the interaction between CRM1 and the nuclear export signal (NES) of the cargo.<sup>8b</sup> To test if anguinomycins C and D and the prepared derivatives could also inhibit this process, we investigated how treatment of cells with these products influences the intracellular localization of the human protein Rio2. This protein is a cytoplasmic protein kinase, which is exported from the nucleus to the cytoplasm by CRM1.<sup>17,32</sup> Inhibition of CRM1-mediated transport results in an accumulation of the Rio2 protein in the nucleus. HeLa cells were incubated with different concentrations of anguinomycin C, anguinomycin D, and derivatives for 2 h and then fixed with paraformaldehyde. LMB was used as a standard reference. After treatment, the localization of Rio2 was determined by indirect immunofluorescence analysis using a specific antibody directed to human Rio2.

Both anguinomycins C and D caused a strong accumulation of the Rio2 protein in the nucleus and displayed activity similar to that of the standard reference LMB, whereas in solvent-treated control cells the Rio2 protein was localized in the cytoplasm (Figure 2A and C). The results confirmed that both anguinomycins C and D are potent inhibitors of CRM1-mediated nucleocytoplasmic transport. Both anguinomycins C and D displayed partial inhibition at 5 nM and reached full inhibition at 10 nM. These values are comparable to those of LMB, which fully inhibits nucleocytoplasmic transport above 1 nM (Figure 2C).

Very interesting results were obtained for the  $\alpha,\beta$ -unsaturated aldehyde 44 and for lactone 4. The results show that aldehyde 44 completely blocks CRM1-dependent nuclear export at 50 nM, with partial inhibition already observable at 25 nM (Figure 2A). This compound displays the same side chain as anguinomycins C and D, but the lactone has been replaced by the  $\alpha,\beta$ -unsaturated aldehyde. Even though this replacement results in a 5-fold loss in activity, compound 44 can still be considered highly active, as it completely blocks CRM1 at 50 nM concentration. Even more surprising was the high activity displayed by product 4, which contains a truncated polyketide chain. The compound caused the accumulation of the Rio2 protein in the nucleus at 25 nM (Figure 2A). This result highlights the fundamental role of the  $\alpha,\beta$ -unsaturated lactone in the inhibition of CRM1-mediated nucleocytoplasmic transport, supporting the hypothesis that the side chain mainly plays a role in the molecular recognition and modulation of the selectivity. Even though compound 4 was a drastic simplification of the natural anguinomycins C and D, the activity decreased only marginally. From the synthetic point of view, lactone 4

(32) (a) Rouquette, J.; Choesmel, V.; Gleizes, P. E. *EMBO J.* **2005**, *24*, 2862–2872. (b) Zemp, I.; Wild, T.; O'Donohue, M.-F.; Wandrey, F.; Widmann, B.; Gleizes, P.-E.; Kutay, U. *J. Cell Biol.* **2009**, *185*, 1167–1180.



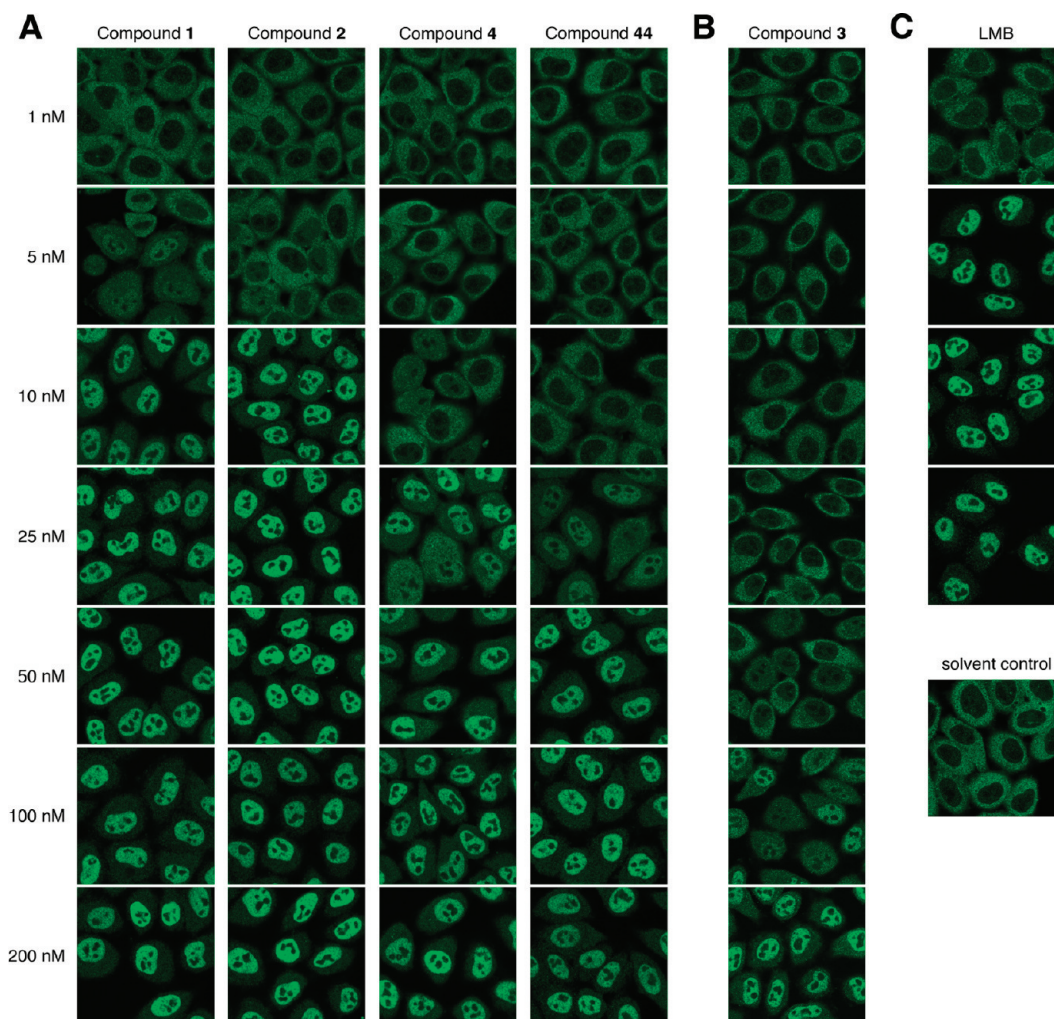


**Figure 2.** Anguinomycins C and D and different derivatives block CRM1-mediated nuclear export in vivo. HeLa cells were incubated with the respective compounds for 2 h at 37 °C. Cells were then fixed in 4% paraformaldehyde, and human Rio2 protein was detected by indirect immunofluorescence analysis using a Rio2-specific antibody. Pictures were taken using a Leica confocal microscope. (A) Inhibition of CRM1-dependent nuclear export of Rio2 in HeLa Cells by anguinomycins C (1) and D (2), compounds 4 and 44. (B) Inhibition of CRM1-dependent nuclear export of Rio2 in HeLa Cells by 3. (C) LMB served as standard reference; incubation with the solvent EtOH (1% v/v) served as negative control.

would be much easier to prepare than the natural compounds, resulting in a gain of time and resources. To understand on an atomic level the reasons for LMB/anguinomycin binding, we carried out modeling studies on the recently published structures of CRM1.<sup>10</sup>

**Modeling of the Interaction between LMB and CRM1.** In 1999, Kudo and colleagues demonstrated that the natural product leptomycin B (LMB) inhibits CRM1 through selective alkylation of a cysteine residue.<sup>9a,b</sup> Earlier in 2009, two X-ray structures of full-length mouse and human CRM1 have been published,<sup>10a,c</sup> which reveal that the reactive cysteine (Cys 528 in human CRM1) locates in a hydrophobic groove responsible for binding of nuclear export signals (NES), as shown in the CRM1–SNUPN complex (Figure 3). The NES binding site of CRM1 is very similar in the two structures with a rmsd of 0.31 Å (see Supporting Information Figure 1). In the following, we investigated how LMB and other compounds tested above bind to and interact with CRM1.

Molecular modeling of covalent inhibitors is considered challenging because the binding energy results from both covalent and noncovalent interactions between the protein and

the inhibitor.<sup>33</sup> Current docking programs capture noncovalent interactions well, but they are largely incapable of estimating the binding energy associated with the formation of a covalent bond between the protein and the inhibitor. An additional challenge is the flexible structure of LMB, which can adopt a large number of possible conformations. However, covalent binding also simplifies modeling because it introduces an anchor point that reduces the number of orientations to be evaluated.

We modeled the LMB binding pose manually and optimized its conformation by an all-atom energy minimization using PLOP.<sup>34</sup> We found that the shape and the electrostatic properties of the CRM1 binding pocket and the rigid parts of the inhibitor restrict the binding mode of LMB to a large extent. Our models suggest a mechanism for inhibitor binding and help to explain why only certain derivatives bind to CRM1. They could be useful for the design of new analogues.

We started with the modeling of the LMB–CRM1 complex at Cys 528, which makes a covalent bond with the lactone ring of LMB. Our first observation was that, due to steric restraints,

(33) Lindvall, M. K. *Curr. Pharm. Des.* **2002**, 8, 1673–1681.

(34) Kalyanaraman, C.; Bernacki, K.; Jacobson, M. P. *Biochemistry* **2005**, 44, 2059–2071.



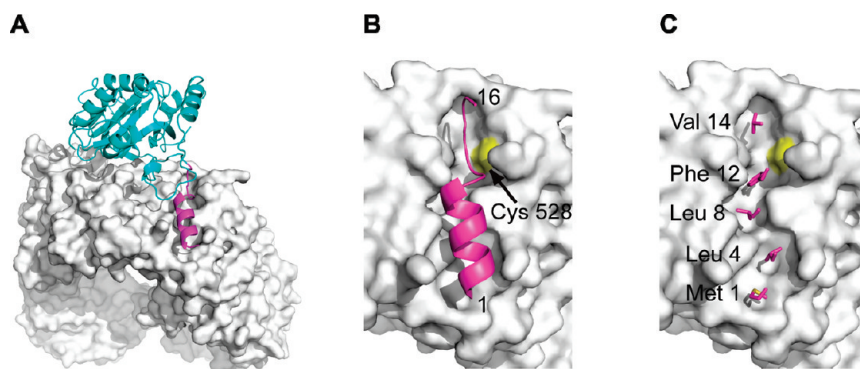


**Figure 3.** X-ray structure of the CRM1–SNUPN complex.<sup>10a</sup> (A) CRM1 is depicted as a surface model in white. SNUPN is displayed as ribbon representation in cyan and magenta. (B) Close-up view on the N-terminal nuclear export signal (NES) of SNUPN (residues 1–16). Leptomycin B binds to Cys 528, which lies in a hydrophobic groove of CRM1. The position of the sulfur atom of Cys 528 is highlighted in yellow. (C) Hydrophobic residues of the SNUPN NES (only side chains shown) define five pockets in the CRM1 groove.

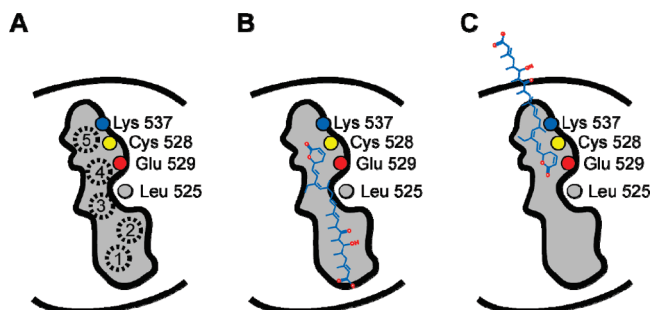


**Figure 4.** Cartoon representations of the CRM1 binding groove and potential orientations of LMB in the binding pocket. Colored circles indicate the location of important residues close to the reactive cysteine 528. (A) The CRM1 groove has five pronounced hydrophobic pockets, displayed by dashed rings. (B) Orientation 1: LMB occupies pockets one to four. (C) Orientation 2: LMB occupies pockets four and five, but does not fit entirely into the binding groove.

LMB can fit only in two orientations into the binding groove of CRM1. CRM1 has five pockets that bind the hydrophobic SNUPN residues (Figures 3C and 4A).<sup>10</sup> Either LMB interacts with pockets one up to four of CRM1 (orientation 1, Figure 4B), or LMB occupies pockets four and five (orientation 2, Figure 4C). We favor orientation 1 over 2 because LMB has not enough space to fit entirely into the groove in orientation 2. In addition, orientation 1 allows clearly more contacts between LMB and CRM1.

Structural analysis of the local environment of Cys 528 provides further support for orientation 1 (Figure 5A). In the course of a Michael addition, a negative charge on the lactone O atom (enolate) is generated. In orientation 2, that enolate would point toward the carboxylate group of Glu 529 and apolar Leu 525. Both of these interactions are unfavorable. On the contrary, in orientation 1, the enolate points toward free space in pocket five, and there is Lys 537 nearby, which could stabilize the negative charge in the transition state. Based on proximity, Glu 529 and Lys 537 are possible candidates as base-catalysts of the reaction. Both residues are 100% conserved among nuclear export proteins.

Our next finding about the lactone ring concerns stereoselectivity of the Michael addition reaction. The thiol of Cys 528 can attack the unsaturated lactone ring of LMB from two different faces. The LMB-adduct has a new stereogenic center at carbon C3 (see Figure 6D for atom numbering). To investigate the configuration of the LMB adduct at C3, we modeled both the (*R*) and the (*S*) stereoisomers into the CRM1 binding pocket.

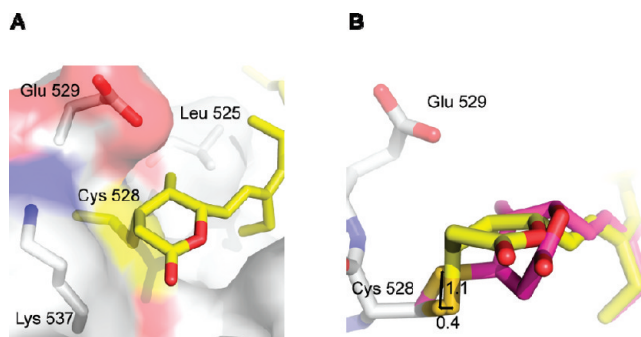


**Figure 5.** The local environment of Cys 528 orients the lactone ring of LMB. (A) Cys 528 is covalently bonded to the lactone ring in the LMB adduct model. Glu 529 and Lys 537 are two charged amino acids in close proximity of Cys 528. Glu 529 appears to be ideally placed to act as a “general base catalyst” in the Michael reaction, while Lys 537 could stabilize a negative charge in the lactone ring in the transition state. (B) Comparison of the crystallographic Cys 528 (depicted in gray) with two possible LMB adduct stereoisomers. Carbon atoms are displayed in yellow and magenta for the (*S*) and (*R*) configurations.

The results after the energy minimization are shown in Figure 5B. To fit the lactone ring in the (*R*) configuration, the S atom of cysteine 528 has to move by 1.1 Å respective to the crystal structure. The lactone ring is easier to accommodate in the (*S*) configuration into the CRM1 pocket because only a small movement of 0.4 Å is necessary. However, this prediction of the absolute configuration is not absolute because it has been modeled into a rigid receptor structure.

After the determination of the lactone ring orientation, modeling of the hydrophobic tail of LMB was straightforward. In the modeling of the tail, we strived toward burying hydrophobic LMB entities as much as possible in the groove. The conjugated diene part of callistatin, a LMB analogue, has been shown to be essential for binding.<sup>35</sup> We concluded therefore that this group makes specific interactions with the groove.

The final models for LMB and the small, but still active compound **4** are presented in Figure 6A and B. Both are shown in orientation 1 and (*S*) configuration for carbon C3, respectively. LMB fills up most of the groove that serves as the molecular recognition site for NES sequences of CRM1 export substrates/ (CRM1) cargo proteins. Within the limitations of rigid body

(35) Murakami, N.; Sugimoto, M.; Nakajima, T.; Kawanishi, M.; Tsutsui, Y.; Kobayashi, M. *Bioorg. Med. Chem.* **2000**, *8*, 2651–2661.

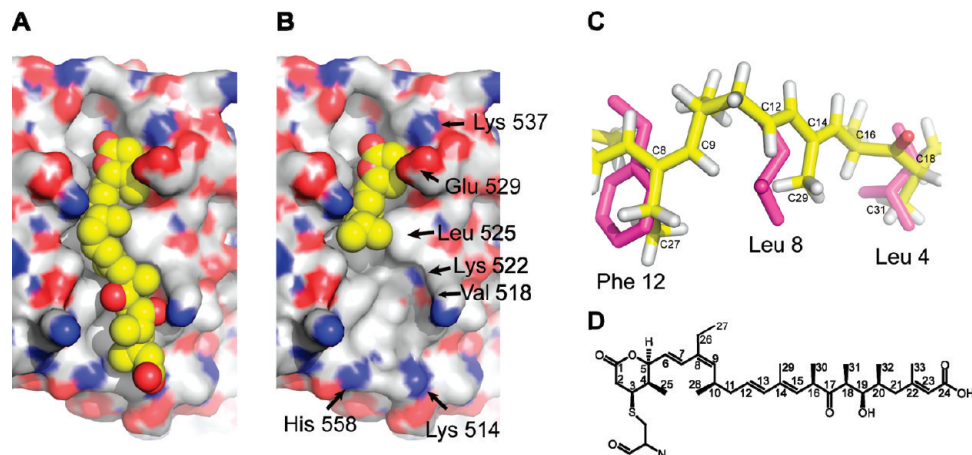


**Figure 6.** Models of CRM1–inhibitor complexes. CRM1 carbons, oxygens, and nitrogen are in gray, red, and blue, respectively. Inhibitors depicted with yellow carbon atoms. (A) Sphere model of Leptomycin B adduct. (B) Sphere model of compound **4** adduct. (C) Superposition of LMB adduct with NES residues of SNUPN. LMB depicted in yellow with hydrogens, SNUPN residues in magenta. (D) Atom numbering of LMB adduct, according to ref 5.

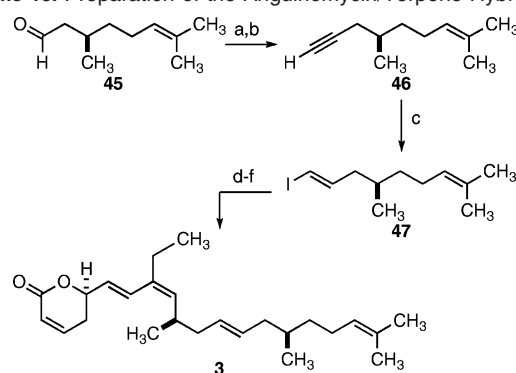
modeling, we think that our model of LMB may be accurate up to carbon atom C15: as described above, steric restraints of the pocket and the arrangement of the charged amino acids Glu 529 and Lys 537 direct the orientation of the lactone and place it between pockets four and five. After the lactone, LMB contains two conjugated dienes, which are rigid stretches in the molecule. Those fit between pockets two and four. Between the dienes, three rotatable bonds between C9 and C12 allow a necessary turn in the bottleneck of the groove, near Leu 525. The ethyl group at C8 has been shown to be important for cytotoxicity;<sup>35</sup> it protrudes deeply into pocket four and mimics thereby phenylalanine 12 from the SNUPN NES (Figure 6C). Also, the methyl groups C29 and C31 mimic hydrophobic SNUPN side chains. The part of the LMB molecule after the two conjugated dienes (C16–C24) is sterically less restricted in the groove and occupies pockets one and two. Seven successive rotatable bonds make this part very flexible. We can only speculate that the keto and hydroxyl groups of LMB may interact with a patch of polar groups between CRM1 residues Val 518 and Lys 522. The terminal carboxyl group could make favorable electrostatic interactions either with His 558 or Lys 514, two positively charged residues near pocket one. Compound **4** is obviously much shorter than LMB but is likely to react via a similar mechanism with CRM1. It retains the ability to block recognition and binding of NES by occupying pockets three and four.

In conclusion, our manual modeling of LMB was guided by the geometry of the ligand and the shape of the CRM1 binding pocket. It yielded plausible and snugly fitting inhibitor conformations rationalizing previous structure–activity experiments. In addition, structural analysis of the local environment of Cys 528 suggests that Glu 529 and Lys 537 are likely taking part in the reaction forming the covalent bond.

#### Synthesis and Evaluation of Anguinomycin/Terpene Hybrid.

At the outset of the research program, we wanted to evaluate the hypothesis whether the polyketide chain of anguinomycin mimics the leucine-rich nuclear export signal (NES) of cargo proteins. This helical peptide NES region features hydrophobic amino acids and has been postulated to weakly interact with CRM1.<sup>11</sup> This hypothesis is supported by the modeling studies discussed above, where the tail of LMB/anguinomycin snugly fits into the binding groove. Therefore, replacement of the polyketide chain by a simpler hydrophobic moiety was desired, and the corresponding compound **3**, which can be considered a hybrid between anguinomycin and a terpene, was targeted.

#### Scheme 10. Preparation of the Anguinomycin/Terpene Hybrid<sup>a</sup>



<sup>a</sup> Reagents and conditions: (a)  $\text{CBr}_4$ ,  $\text{PPh}_3$ , 2,6-lutidine,  $\text{CH}_2\text{Cl}_2$ , 0 °C, 2 h, 91%. (b)  $n\text{BuLi}$ , THF, –78 °C to room temperature then  $\text{NH}_4\text{Cl}$ . (c)  $\text{Cp}_2\text{ZrHCl}$ , 0 °C → room temperature, THF, 1 h, then –78 °C,  $\text{I}_2$  (87% over two steps). (d) **21**, 9-MeO-9-BBN (1.0 M in hexane),  $t\text{BuLi}$  (1.5 M in pentane),  $\text{Et}_2\text{O}$ , then THF, –78 °C → room temperature, 1 h, then **47**,  $\text{Pd}(\text{dppf})\text{Cl}_2 \cdot \text{CH}_2\text{Cl}_2$  (5 mol %),  $\text{AsPh}_3$  (15 mol %),  $\text{CsCO}_3$ ,  $\text{H}_2\text{O}$ , DMF, room temperature, overnight, 87%. (e) PPTS, acetone/water (3/1), room temperature, 2 h. (f) PCC, 4 Å MS,  $\text{CH}_2\text{Cl}_2$ , room temperature (53% over two steps).

Citronellal (**45**) was converted to the corresponding dibromoolefin<sup>36</sup> followed by transformation to the alkyne **46** via the Fritsch–Buttenberg–Wiechell rearrangement.<sup>37</sup> The selective formation of the (*E*)-iodoolefin **47** was achieved by hydrozirconation using Schwartz reagent and quenching with  $\text{I}_2$ .<sup>38</sup> All attempts toward the formation of compound **47** via Takai olefination<sup>28</sup> from citronellal were unsuccessful due to the lack of selectivity. The coupling of the side-chain to the alkyl iodide **21** was achieved using the previously described  $\text{sp}^3$ – $\text{sp}^2$  Suzuki cross-coupling. Finally, removal of the isopropyl group and oxidation to the lactone using PCC gave the desired analogue **3** (Scheme 10).

To analyze whether **3** is capable of blocking CRM1-mediated nuclear export, we incubated HeLa cells with increasing concentrations of this compound and analyzed the localization of human Rio2 protein (Figure 2B). Interestingly, **3** displayed full inhibition of CRM1-dependent nuclear export at 200 nM,

(36) Corey, E. J.; Fuchs, P. L. *Tetrahedron Lett.* **1972**, 13, 3769–3772.

Molander, G. A.; Yokoyama, Y. *J. Org. Chem.* **2006**, 71, 2493–2498.

(37) Minatti, A.; Dötz, K. H. *J. Org. Chem.* **2005**, 70, 3745–3748.

(38) Huang, Z.; Negishi, E. *Org. Lett.* **2006**, 8, 3675–3678.

with partial inhibition of export starting at 25 nM. This result demonstrates that the polyketide chain of anguinomycins C and D can be replaced by a hydrophobic moiety without a strong loss in activity. Moreover, the observed reduction in activity for **3** might be partially due to an increased capability of the compound to dissolve into lipid bilayers, as its hydrophobic moiety strongly resembles the apolar parts of phospholipids. This might significantly reduce the active concentration of the compound present within the cell.

## Discussion

The biological results obtained in this work can be compared to the SAR investigation of other groups on related compounds. Kobayashi and co-workers reported biological investigations on callistatin and its derivatives,<sup>39</sup> proving the fundamental importance of the lactone fragment for the activity. The same studies showed that modifications of the polyketide chain cause a loss in activity of about 1 order of magnitude as compared to the natural callistatin. In addition, inversion of configuration at C(5) caused a 350-fold loss in activity. Kalesse and co-workers performed similar investigations on ratjadone,<sup>40</sup> showing again that the lactone was crucial for activity. Inversion of configuration at C(10) resulted in a complete loss of activity. Recently, Mutka and co-workers reported new derivatives of LMB displaying the same potency as the parent compound, but with a higher selectivity between normal and cancer cells.<sup>14e</sup> Structure–activity relationship studies performed on anguinomycins C and D and their derivatives as described above were in agreement with the literature. The high activity of compound **4** (25 nM) can be explained by the fact that this derivative is a shortened version of the parent compound, which lacks the polyketide chain but still contains the important lactone moiety. This is an interesting finding, as for many natural products, omission of more than one-half of the C skeleton often leads to complete loss of bioactivity.

## Conclusion

The need to find more selective inhibitors of nucleocytoplasmic transport and the unveiled structure of anguinomycins C and D prompted us to develop a synthesis for these natural products. With its six unknown stereogenic centers, the lactone ring, the two diene systems, and the polyketide chain, anguinomycins presented a challenging target for total synthesis. The

first total syntheses of anguinomycins C and D were achieved in total 29 steps with a longest linear sequence of 18 steps from (*R*)-4-isopropyl-5,5-diphenyloxazolidin-2-one and with an overall yield of 6.7% and 6.0%, respectively. Noteworthy steps included: (1) the Cr(III)-catalyzed hetero Diels–Alder giving straightforward access to the dihydropyran ring in high yield and selectivity and (2) the Negishi cross-coupling under stereoinversion that furnished the *cis* product for both anguinomycins C and D from a common starting material. This exemplifies the potential of this reaction in total synthesis, and we are confident that more applications will be demonstrated in the future. The Seebach modification of the Evans auxiliary demonstrated its utility for the synthesis of polyketide chains with regard to yield, selectivity, and simplicity. The total synthesis also definitively established the absolute configuration of anguinomycins C and D as (5*R*,10*R*,16*R*,18*S*,19*R*,20*S*).

Following the total syntheses of the two natural compounds, we investigated the biology of these products and more precisely the mode of action and the structure–activity relationships. Several derivatives were prepared and submitted for biological evaluation. The results confirmed the crucial importance of the lactone ring for the activity and also that the activity can be modulated by changing the side chain, which mainly plays a role in the molecular recognition. Both anguinomycins C and D displayed a strong inhibition of the CRM1-mediated nucleocytoplasmic transport at 10 nM, confirming their powerful activity. Moreover, the truncated analogue **4** that caused accumulation of the Rio2 protein in the nucleus at 25 nM was obtained. This compound represents a drastic simplification of the parent natural product, and it maintained strong activity despite omission of more than one-half of the carbon skeleton. This truncated analogue **4** can be considered a starting point for the development of similar, short analogues of LMB and anguinomycins and can thus contribute to the search for more powerful and selective nucleocytoplasmic transport inhibitors for cancer treatment.

**Acknowledgment.** This work is dedicated to Prof. Eric N. Jacobsen on the occasion of his 50th birthday. K.G. is a European Young Investigator (EURYI). We thank the SNF for support of this work (3100AO-118053, PBZHP3-123277, 200021-115918/1, and PE002-117136/1).

**Supporting Information Available:** Experimental procedures, characterization, spectra, biological, and modeling methods. This material is available free of charge via the Internet at <http://pubs.acs.org>.

JA9097093

(39) Murakami, N.; Sugimoto, M.; Kobayashi, M. *Bioorg. Med. Chem.* **2001**, *9*, 57–67.

(40) Kalesse, M.; Christmann, M.; Bhatt, U.; Quitschalle, M.; Claus, E.; Saeed, A.; Burzlaff, A.; Kasper, C.; Haustedt, L. O.; Hofer, E.; Scheper, T.; Beil, W. *ChemBioChem* **2001**, *2*, 709–714.